Electronic Supplementary Material (ESI) for Physical Chemistry Chemical Physics

Experimentally measured permanent dipoles induced by hydrogen bonding. The Stark spectrum of indole-NH_3.

Adam J. Fleisher,[†] Justin W. Young, and David W. Pratt*

Department of Chemistry, University of Pittsburgh, Pittsburgh, PA 15260

*Corresponding author: pratt@pitt.edu

[†]Present address: JILA, National Institute of Standards and Technology and University of Colorado, Boulder, Colorado 80309

SUPPORTING INFORMATION

S.1. Simulation of *E* band rotational structure.

Below, estimated inertial parameters for the *E* band of indole-NH_3 are listed in Table S-1. These parameters were used to simulate the *E* band, which is shown in red along with the fit *A* band (blue) in Fig. S-1. From many simulations of the E band, we estimate the perturbation terms due to internal rotation to be $D_a \approx 3900 \pm 400$ cm^{-1} and $D_b \approx 900 \pm 100$ cm^{-1} in both electronic states.

Table S-1. Inertial parameters used to simulate the *E* band of InA shown in Fig. S-1.

State	Parameter	Perturbed Asymmetric Rotor
S_0	*A* (MHz)	2067
	B (MHz)	945
	C (MHz)	652
	ΔI (uÅ^2)	-4.2
	κ	-0.6
	D_a (MHz)	4106
	D_b (MHz)	963
S_1	*A* (MHz)	1976
	B (MHz)	980
	C (MHz)	657
	ΔI (uÅ^2)	-1.9
	κ	-0.5
	D_a (MHz)	4186
	D_b (MHz)	876
	Origin (cm^{-1})	35012.3
	Linewidth L/G (MHz)	25/25 ± 2
	T_{rot} (K)	5 ± 1
	Transition Moment *a*/*b*/*c*	0/100/0 ± 5

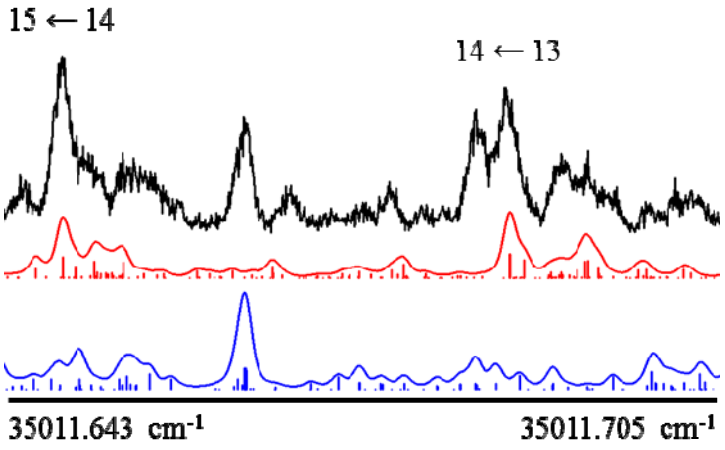

Figure S-1. Above, the experimental spectrum of indole-NH_3 is shown in black, the simulated *E* band is shown in red, the fit *A* band shown in blue. Two *E* band transitions are labeled by their *J′* ← *J″* quantum numbers, and involve transitions between levels with $K_a < 2$.

S.2. Barrier height analysis.

The effective inertial defect ΔI_{eff} measured for the *A* subband of InA contains second-order contributions from the coupling of torsion and overall rotation. The ΔI_{eff} of the *A* subband is related to the effective rotational constants *via*

Equation S-1

$$\Delta I_{off} = \frac{k}{C_{eff}} - \frac{k}{A_{eff}} - \frac{k}{B_{eff}}$$

where k = 505379.005 uÅ^{2}MHz. The ammonia molecule lies in the *ab* plane of the InA complex at hydrogen bond angles of 32° in S_0 and 36° in S_1. Therefore, there is no projection of the internal rotation axis of NH_3 onto the *c* inertial axis of the complex, and the effective rotational constants are related to the static rotational constants *via*

Equation S-2

$$A_{\text{eff}} = A + FW_{v\sigma}^{(2)}\rho_a^2$$

Equation S-3

$$B_{\text{eff}} = B + FW_{v\sigma}^{(2)}\rho_b^2$$

Equation S-4

$$C_{\text{eff}} = C$$

Above, F is the internal rotor constant in MHz, and can be calculated from the known moment of inertia of NH_3 (I_α),[1] the projection of the internal rotor axis onto the inertial axes of the system, and a reducing factor r.

Equation S-5

$$F = \frac{k}{rI_\alpha}$$

Equation S-6

$$r = 1 - \left[\frac{\lambda_a^2 I_\alpha}{I_a} - \frac{\lambda_b^2 I_\alpha}{I_b} - \frac{\lambda_c^2 I_\alpha}{I_c}\right]$$

In InA, we calculated F'' = 188.0 GHz in S_0 and F' = 187.7 GHz in S_1. Additionally, ρ_a and ρ_b are the projection of I_α onto either the a or b inertial axes of InA, and are calculated using the direction cosines λ_g and Eqs. S-7 and S-8.

Equation S-7

$$\rho_a = \frac{\lambda_a I_\alpha}{I_a}$$

Equation S-8

$$\rho_b = \frac{\lambda_b I_\alpha}{I_b}$$

In defining the above equations, our goal is to estimate the static rotational constants A, B, and C in order to calculate values of $W^{(2)}$ in each electronic state. In Table 2 of the main text, the optimized static structures of InA consistently yield inertial defect values of ΔI_{stat} = -2.67 uÅ^2. Therefore, the static rotational constants are related to ΔI_{stat} *via*

Equation S-9

$$\Delta I_{stat} = \frac{k}{C} - \frac{k}{A} - \frac{k}{B}$$

where A, B, and C are defined in Eqs. S-2 through S-4. If we rearrange Eqs. S-2 through S-4 and substitute for the static rotational constants, it becomes possible to vary $W^{(2)}$ to reproduce ΔI_{stat} in each electronic state.

Equation S-10

$$\Delta I_{stat} = \frac{k}{C_{eff}} - \frac{k}{A_{eff} - FW_{00}^{(2)}\rho_a^2} - \frac{k}{B_{eff} - FW_{00}^{(2)}\rho_b^2}$$

The $W^{(2)}$ values determined in this way are related to the barrier height[2,3] *via* Herschbach's equations[4] and available data tables.[5] For the ground state of InA, we calculated V_3'' = 44 cm^{-1}. In the excited state, we calculated a slightly larger barrier height of V_3' = 48 cm^{-1}. This change in

barrier height upon excitation predicts an *E*-*A* band tunneling splitting of -9930 MHz, in excellent agreement with the experimental estimate of ~9900 MHz.

We have checked this procedure by completing the same *A* subband analysis for NH_3 internal rotors previously analysis using high resolution electronic spectroscopy.[6-8] Table S-2 lists the V_3 barrier heights calculated from the *A* subband inertial defect as compared to the more accurate V_3 values calculated from a direct rotational fit of the *E* subbands, which provide the first-order perturbation coefficients $W^{(1)}$. Clearly, the ΔI analysis consistently overestimates the V_3 barrier heights. We therefore conclude that the V_3 barriers to hindered internal rotation of NH_3 in the InA complex are less than $V_3'' = 44$ and $V_3' = 48$ cm^{-1}, respectively.

Table S-2. Predicted V_3 barrier heights (cm^{-1}) using *A* subband ΔI_{eff} values ($uÅ^2$) from select NH_3 complexes. All predicted V_3 values overestimate the barrier height as compared to V_3 calculated from the first-order perturbation coefficients $W^{(1)}$ determined by fitting the respective *E* subbands.

State	Parameter	*c*2HNA[a]	*t*2HNA[b]	*t*1HNA[c]	*t*HQA[d]	InA[e]
S_0	ΔI_{eff} from *A* band	-0.936	-1.262	-1.215	-0.980	+0.27
	V_3 from ΔI_{eff}	71.3	84.1	81.5	74.4	44
	V_3 from *E* band	41.1	34.2	39.9	35.5	--
S_1	ΔI_{eff} from *A* band	-1.286	-1.443	-1.117	-1.381	+0.04
	V_3 from ΔI_{eff}	83.4	91.5	77.9	88.8	48
	V_3 from *E* band	53.8	58.2	46.5	58.8	--

[a] *cis*-β-naphthol-NH_3 (Ref. 6).
[b] *trans*-β-naphthol-NH_3 (Ref. 6).
[c] *trans*-α-naphthol-NH_3 (Ref. 7).
[a] *trans*-hydroquinone-NH_3 (Ref. 8).
[e] This work.

Finally, we have calculated the theoretical inertial defect values for the complexes listed in Table S-2 by requiring the reproduction of each V_3 barrier height calculated from each *E* subband fit (labeled ΔI_{theor}). The following equation, which removes both static and measured

inertial defect contributions from the theoretical values, leaves a barrier-dependent inertial defect term ΔI_{cor}.

Equation S-11

$$\Delta I_{theor} = \Delta I_{exp} + \Delta I_{stat} + \Delta I_{cor}$$

This ΔI correction factor appears linearly related to the measured V_3 barrier heights over the range of 30-65 cm^{-1}, as shown in Fig. S-2. This interesting observation requires more attention in order to understand and interpret the physical meaning and predictive capabilities of such a linear relationship, which appears to describe the barrier height dependence of zero-point vibration on the measured *A* band inertial defects.

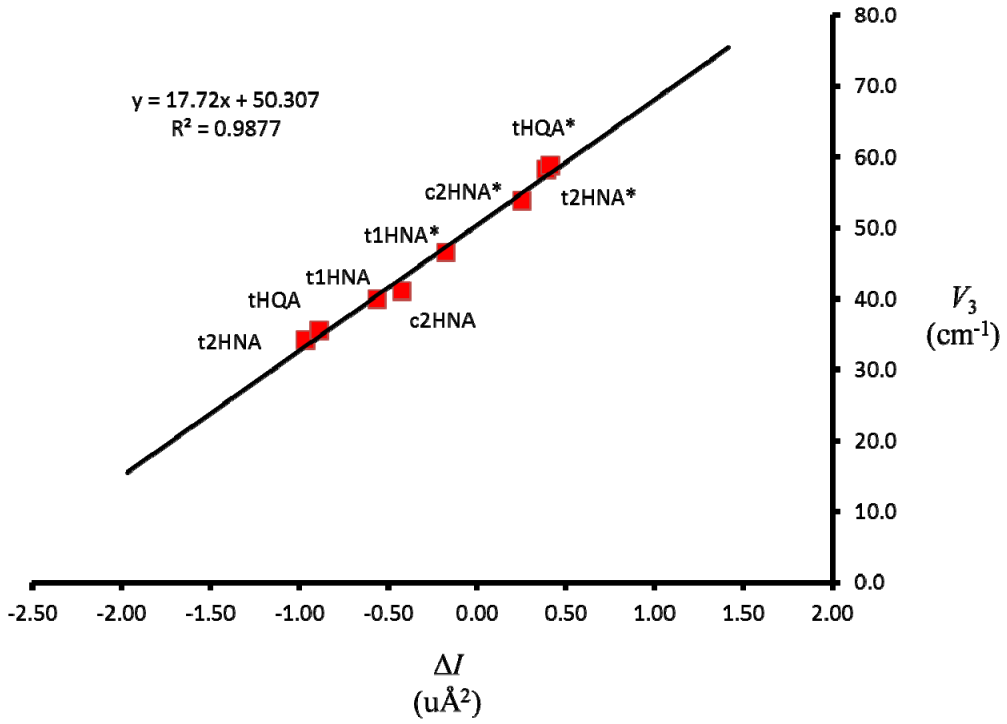

Figure S-2. Plot of V_3 *vs*. ΔI_{cor} for the four complexes listed in Table S-2. A best-fit trend line equation is shown in the top left corner. An asterisk (*) indicates an excited S_1 state data points.

S.3. Electrostatic dipole decomposition.

S.3.1. Principal axes transformation.

The absolute position of the ammonia moiety within the InA inertial frame, as well as the inertial frame of indole, was determined using the analysis set forth by Kraitchman[9] and Rudolph,[10] and discussed in detail by Gordy and Cook.[11] Using the experimentally determined rotational constants *A*, *B*, and *C*, the moments of inertia in the principal axes system can be determined using Eq. S-12.

Equation S-12

$$I_a = \frac{h}{8\pi^2 cA}$$

Eq. S-12 is cyclic in *A*, *B*, and *C*. The planar moments of inertia X, Y, and Z are defined by

Equation S-13

$$X = \frac{-I_a + I_b + I_c}{2}$$

which is also cyclic in *a*, *b*, and *c*. For a molecule or complex with a plane of symmetry, $Z = 0$.

In order to transform between the indole and InA coordinate systems, a transformation matrix was defined which rotates a vector $\mathbf{r}'$ into another vector $\mathbf{r}$. From this point forward, primed vectors and positions will represent the coordinate system of the inA complex (substitute). Unprimed vectors and positions will represent the coordinate system of indole (the parent). The transformation matrix $\mathbf{R}$ is defined as

Equation S-14

$$\vec{r}' = R\vec{r} + \vec{t}$$

where **t** is a necessary translation when the center of the parent and substitute principal axes systems are not identical. When transforming the vector direction of a dipole moment, only the transformation matrix **R** is necessary.

When the aforementioned isotopic substitution occurs within a molecular plane of symmetry, the absolute positions within the parent frame are

Equation S-15

$$|x| = \left[\frac{(X' - X)(Y' - X)}{\mu_m(Y - X)}\right]^{1/2}$$

Equation S-16

$$|y| = \left[\frac{(X' - Y)(Y' - Y)}{\mu_m(X - Y)}\right]^{1/2}$$

and within the substitute frame are

Equation S-17

$$|x'| = \left[\frac{(X - X')(Y - X')}{\mu'_m(Y' - X')}\right]^{1/2}$$

Equation S-18

$$|y'| = \left[\frac{(X - Y')(Y - Y')}{\mu'_m(X' - Y')}\right]^{1/2}$$

where μ_m (μ'_m) is the reduced mass of the isotopic substitution (removal of isotopic substitution)

Equation S-19

$$\mu_m = \frac{M\Delta m}{M + \Delta m}$$

Equation S-20

$$\mu'_m = \frac{M'\Delta m'}{M' + \Delta m'}$$

with M (M') as the total mass of the parent (substitute) and Δm as the difference in mass between the substitute and the parent ($\Delta m' = -\Delta m$). Using the above equations, **R** is defined for a planar substitution as

Equation S-21

$$R = -\Delta m \begin{Bmatrix} \frac{xx'}{X - X'} & \frac{xy'}{X - Y'} & 0 \\ \frac{yx'}{Y - X'} & \frac{yy}{Y - Y'} & 0 \\ 0 & 0 & \frac{-1}{\Delta m} \end{Bmatrix}$$

Following the definition set out in Eq. S-14, the transpose of Eq. S-21, **R′** was used to express the dipole moments of indole in Table 6 of the main text in the inertial frame of InA (Tables S-3 and S-4). Matrix **R** was also used to transform the theoretical polarizability tensor of indole into the inertial frame of InA.

Equation S-22

$$\vec{\mu'} = R'\vec{\mu}$$

Equation S-23

$$\alpha^{I} = R^{t}\alpha R$$

The transformations from the ammonia inertial frame to that of the InA complex required a second transformation matrix based on direction cosines, called **N**. Using Fig. S-3, the transformation matrix **N** is defined as

Equation S-24

$$\vec{\mu}^{I}_{NH_3} = N\vec{\mu}_{NH_3}$$

where

Equation S-25

$$N = \begin{Bmatrix} \cos(90-\theta_{HB}) & 0 & -\cos\theta_{HB} \\ \cos\theta_{HB} & 0 & \cos(90-\theta_{HB}) \\ 0 & -1 & 0 \end{Bmatrix}$$

For InA, θ_{HB} = 32° in S_0 and θ_{HB} = 36° in S_1. These angles were determined using the known Kraitchman positions of the indole amino hydrogen and the ammonia point mass both in the InA inertial frame.

Matrix **N** was also used to transform the quadrupole moment of ammonia into the indole inertial frame by Eq. S-26

Equation S-26

$$\Theta^{I}_{NH_3} = N\Theta_{NH_3}N^{t}$$

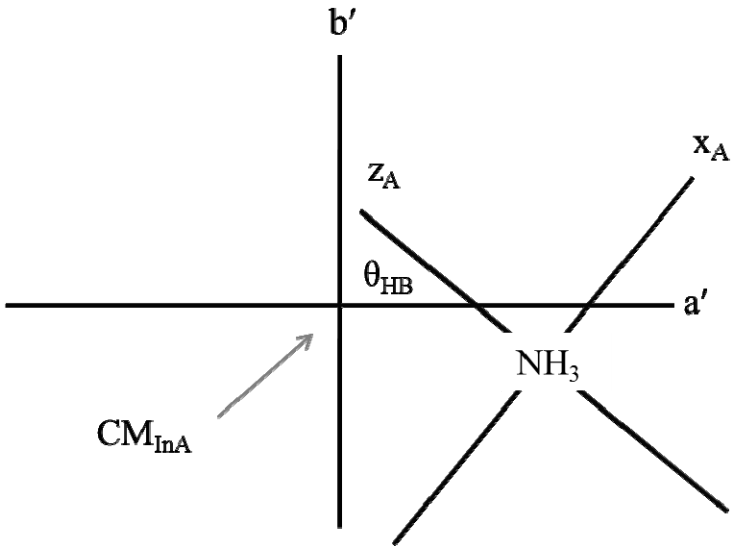

Figure S-3. Representation of the NH_3 principal inertial axes (subscript "A") superimposed onto the indole-NH_3 frame (primed axes) and center of mass (CM).

S.3.2. Interaction energy decomposition.

Intermolecular forces are dominated by both static and time-dependent electronic interactions.[12] Both indole and NH_3 are polar, neutral molecules, and both electrostatic and induced interaction terms are expected to participate in the stabilization of InA in both S_0 and S_1. The electrostatic interaction energy is defined as the interaction between the total dipole moments of indole and NH_3 separated by the known center of mass distance.

Equation S-27

$$E_{el} = \frac{1}{4\pi\varepsilon_0}\left[-\frac{\mu_1\mu_2}{r^3}(2\cos\theta_1\cos\theta_2 - \sin\theta_1\sin\theta_2\cos\phi)\right]$$

The distance *r* is the distance between the center of mass of indole and the center of mass of ammonia, treated as a point mass using the Kraitchman's analysis. The remaining angles and dipoles are defined in Fig. S-4 and listed in Tables S-3 and S-4. Higher order terms, including

dipole-quadrupole and quadrupole-quadrupole were considered small, and therefore not included in this term.

Table S-3. Indole and NH_3 ground state parameters expressed in the InA S_0 coordinate system.

State	Parameter	Indole frame	InA frame	NH_3 frame	InA frame	InA
S_0	μ_a (D)	1.376	1.962	0	1.248	
	μ_b (D)	1.40	0.06	0	0.781	
	μ_c (D)	0	0	1.472	0	
	μ (D)	1.963	1.963	1.472	1.472	
	θ_1 (deg)		58.0			
	θ_2 (deg)				27.7	
	θ_{HB} (deg)					32.0
	r_{CM} (Å)					4.756
	Θ_{aa} (D Å)			1.16	-1.34	
	Θ_{ab} (D Å)			0	1.57	
	Θ_{bb} (D Å)			1.16	0.18	
	Θ_{ba} (D Å)			0	1.57	
	Θ_{cc} (D Å)			-2.32	1.16	
	Θ (D Å)			-3.12	-3.12	
	α_{aa} (Å^3)	17.71	15.62			
	α_{ab} (Å^3)	0.11	2.07			
	α_{bb} (Å^3)	13.57	15.66			
	α_{ba} (Å^3)	0.11	2.07			
	α_{cc} (Å^3)	4.36	4.36			
	α (Å^3)	1047	1047			
	$\mu_{pol,a}$ (D)					0.49
	$\mu_{pol,b}$ (D)					0.28
	μ_{pol} (D)					0.56
	$\mu_{CT,a}$ (D)					1.00
	$\mu_{CT,b}$ (D)					0.03
	μ_{CT} (D)					1.00
	d (Å)					3.07
	Q (e)					0.06

Table S-4. Indole (excited state) and NH_3 (ground state) parameters expressed in the InA S_1 coordinate system.

State	Parameter	Indole frame	InA frame	NH_3 frame	InA frame	InA
S_1	μ_a (D)	1.556	1.809	0	1.191	
	μ_b (D)	1.01	0.412	0	0.865	
	μ_c (D)	0	0	1.472	0	
	μ (D)	1.963	1.855	1.472	1.472	
	θ_1 (deg)		75.3			
	θ_2 (deg)				26.5	
	θ_{HB} (deg)					36.0
	r_{CM} (Å)					4.660
	Θ_{aa} (D Å)			1.16	-1.12	
	Θ_{ab} (D Å)			0	1.66	
	Θ_{bb} (D Å)			1.16	-0.04	
	Θ_{ba} (D Å)			0	1.66	
	Θ_{cc} (D Å)			-2.32	1.16	
	Θ (D Å)			-3.12	-3.12	
	α_{aa} (Å^3)	22.74	19.44			
	α_{ab} (Å^3)	-1.1	4.31			
	α_{bb} (Å^3)	14.19	17.49			
	α_{ba} (Å^3)	-1.1	4.31			
	α_{cc} (Å^3)	4.52	4.52			
	α (Å^3)	1453	1453			
	$\mu_{pol,a}$ (D)					0.57
	$\mu_{pol,b}$ (D)					0.36
	μ_{pol} (D)					0.67
	$\mu_{CT,a}$ (D)					0.96
	$\mu_{CT,b}$ (D)					0.26
	μ_{CT} (D)					1.00
	d (Å)					2.97
	Q (e)					0.07

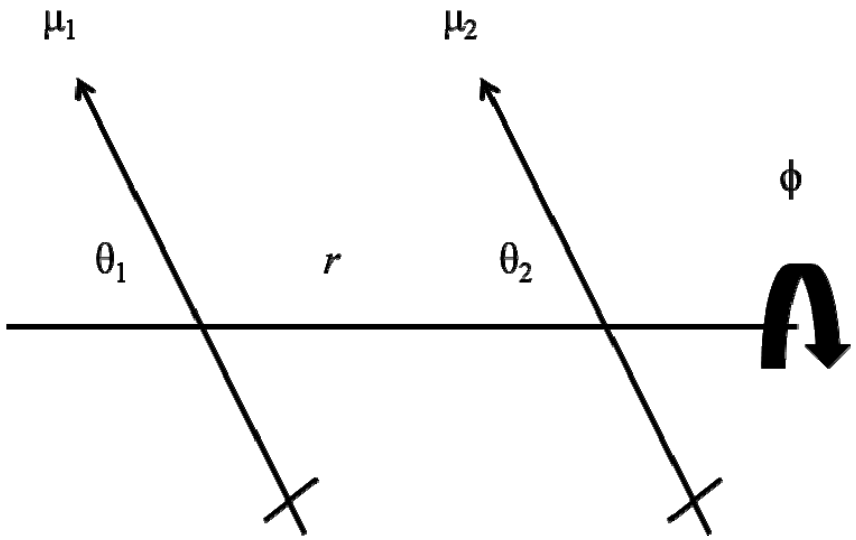

Figure S-4. Definition of dipole angles and center of mass distance used in the electrostatic interaction equations. Subscript "1" is used for bare indole, and subscript "2" is used for NH_3. For the InA complex, $\phi = 0°$.

The induced dipole is comprised of two components: the polarization dipole and the charge transfer dipole. The polarization dipole is defined as the electric field of NH_3 scaled by the polarizability of indole.[13]

Equation S-28

$$\vec{\mu}_{pol} = \alpha \left[\frac{2\vec{\mu}_{NH_3}}{r^3} + \frac{3\Theta_{NH_3}}{r^4} \right]$$

In Eq. S-38, the dipole[14] and quadrupole moments[15] of NH_3 were expressed in the inertial frame of InA as described above. The dipole of NH_3 was expressed as a diagonal 3x3 matrix (the polarizability and quadrupole tensors are also both 3x3), and the polarization-induced dipole moment was taken to be the eigenvalues of the resulting matrix multiplication. The dipole induced on NH_3 by the electric field of indole is considered small, and therefore not included.

The polarization-induced stabilization energy can be calculated from Eq. S-39 and the inclusion of the angle dependence of the NH_3 electric field (E)[12] defined in Fig. S-4. Eq. S-39 makes us of the dipole and quadrupole moment magnitudes, and not vector and tensor components.

Equation S-29

$$E_{pol} = \frac{1}{2}\mu_{pol}E = -\frac{\mu_{pol}}{8\pi\epsilon_0}\left[\frac{(\mu_{NH_3})^2}{r^6}(3\cos^2\theta_2 + 1)\right.$$

$$\left. + \frac{9(\Theta_{NH_3})^2}{4r^8}((3\cos^2\theta_2 - 1)^2 + 4\cos^2\theta_2 \sin^2\theta_2)\right]^{1/2}$$

The charge transfer dipole is defined in Eq. 5 of the main text. The charge transfer dipole was used to calculate the fractional electronic charge separation between the hydrogen bond heavy atoms;[16] both nitrogen atoms in the InA complex. This distance, defined as *d*, was calculated at the M05-2X/aug-cc-pVQZ level to be d = 3.07 Å in S_0. The change in hydrogen bond length upon electronic excitation was measured as -0.1 Å in the main text using Kraitchman's analysis, and therefore d = 2.97 Å in S_1.

Equation S-30

$$\mu_{CT} = Qd$$

Equation S-31

$$E_{CT} = \frac{1}{4\pi\varepsilon_0}\frac{-Q^2}{r}$$

The total stabilization energy relative to that of bare indole in each electronic state was calculated as $E_{rel} = E_{el} + E_{pol} + E_{CT}$. Therefore, the gas phase solvatochromic shift in the $S_1 \leftarrow S_0$ electronic excitation of indole as induced by a single hydrogen bond with NH_3 is

Equation S-32

$$\Delta E_{rel} = E_{rel}^{S_1} - E_{rel}^{S_0} = +20 \text{ cm}^{-1}$$

REFERENCES

1. V. A. Job, N. D. Patel, R. D'Cunha, and V. B. Kartha, *J. Mol. Spectrosc*. 1983, **101**, 48.

2. A. C. Fantoni and W. Caminati, *J. Chem. Soc., Faraday Trans*., 1996, **92**, 343.

3. W. Caminati, J. C. Lopez, S. Blanco, S. Mata, and J. L. Alonso, *Phys. Chem. Chem. Phys*., 2010, **12**, 10230.

4. D. R. Herschbach, *J. Chem. Phys*., 1959, **31**, 91.

5. *Tables Relating to Mathieu Functions*, Columbia University Press, New York, 1951.

6. D. F. Plusquellic, X. -Q. Tan, D. W. Pratt, *J. Chem. Phys*., 1992, **96**, 8026.

7. S. J. Humphrey and D. W. Pratt, *J. Chem. Phys*., 1996, **104**, 8332.

8. S. J. Humphrey and D. W. Pratt, *J. Chem. Phys*., 1997, **106**, 908.

9. J. Kraitchman, *Am. J. Phys*., 1953, **21**, 17-24.

10. H. D. Rudolph, *J. Mol. Spectrosc*., 1981, **89**, 430-439.

11. W. Gordy and R. Cook, L., *Microwave Molecular Spectra*, John Wiley & Sons, New York, 1984.

12. G. C. Maitland, M. Rigby, E. B. Smith, and W. A. Wakeham, *Intermolecular Forces*, Clarendon Press, Oxford, 1981.

13. C. Kang, T. M. Korter and D. W. Pratt, *J. Chem. Phys.*, 2005, **122**, 174301.

14. M. D. Marshall and J. S. Muenter, *J. Mol. Spectrosc*., 1981, **85**, 322.

15. S. G. Kukolich, *Chem. Phys. Lett*., 1970, **5**, 401.

16. A. J. Fleisher, P. J. Morgan, and D. W. Pratt, *J. Chem. Phys*. 2009, **131**, 211101.